



저작자표시-비영리-변경금지 2.0 대한민국

이용자는 아래의 조건을 따르는 경우에 한하여 자유롭게

- 이 저작물을 복제, 배포, 전송, 전시, 공연 및 방송할 수 있습니다.

다음과 같은 조건을 따라야 합니다:



저작자표시. 귀하는 원저작자를 표시하여야 합니다.



비영리. 귀하는 이 저작물을 영리 목적으로 이용할 수 없습니다.



변경금지. 귀하는 이 저작물을 개작, 변형 또는 가공할 수 없습니다.

- 귀하는, 이 저작물의 재이용이나 배포의 경우, 이 저작물에 적용된 이용허락조건을 명확하게 나타내어야 합니다.
- 저작권자로부터 별도의 허가를 받으면 이러한 조건들은 적용되지 않습니다.

저작권법에 따른 이용자의 권리는 위의 내용에 의하여 영향을 받지 않습니다.

이것은 [이용허락규약\(Legal Code\)](#)을 이해하기 쉽게 요약한 것입니다.

[Disclaimer](#)

공학석사 학위논문

소비전력 측정을 통한 밀링 공정의  
가공 모니터링

Monitoring of Milling Processes through  
Measurement of Power Consumption

2019년 2월

서울대학교 대학원

기계항공공학부

류종하

## Abstract

# Monitoring of Milling Processes through Measurement of Power Consumption

Jongha Yu

Department of Mechanical and Aerospace  
Engineering  
The Graduate School  
Seoul National University

Tool condition monitoring is crucial in accurately diagnosing tool wear and detecting or preventing tool failure. 7–20% of total milling–machine downtime is due to tool failure and 3–12% of total processing cost comes from tool change costs. In addition, indirect costs due to poor surface quality can be added with the absence of a monitoring system. Conventional tool monitoring systems are difficult to implement due to high costs or the need for downtime. This thesis proposes a low–cost wireless monitoring system with very little down time for implementation that can deduce the state of the tool with the monitoring of power consumed by a CNC milling machine.

**Keyword :** Power monitoring, Tool condition monitoring, Milling

**Student Number :** 2017–26871

# Table of Contents

<b>Chapter 1. Introduction.....</b>	<b>1</b>
1.1. Study Background .....	1
1.2. Purpose of Research .....	4
<b>Chapter 2. Hardware .....</b>	<b>5</b>
2.1. System Layout.....	5
2.2. System Design.....	6
<b>Chapter 3. Experiments and Results .....</b>	<b>12</b>
3.1. Early Experiments.....	12
3.2. Mathematical Model.....	19
3.3. Machine Learning Model .....	28
3.4. Summary .....	31
<b>Chapter 4. Conclusion.....</b>	<b>32</b>
<b>Reference.....</b>	<b>33</b>
<b>Abstract in Korean .....</b>	<b>37</b>

# List of Figures

<b>Figure 1</b> Monitoring System Layout .....	5
<b>Figure 2</b> Noisy Hall–sensor readings by Arduino of 220 V 60 Hz power supply .....	6
<b>Figure 3</b> Model for Arduino–based monitoring system .	7
<b>Figure 4</b> Optimized algorithm for Arduino.....	9
<b>Figure 5</b> Comparison between Siemens and Arduino monitoring systems for accuracy.....	10
<b>Figure 6</b> Example of a MQTT protocol.....	11
<b>Figure 7</b> Slot milling process repeated 30 times .....	12
<b>Figure 8</b> Power consumption increase with tool wear in slot milling .....	13
<b>Figure 9</b> CAD model of triangular cutting experiment..	14
<b>Figure 10</b> Simulation using CAMotics, a tool path generator .....	14
<b>Figure 11</b> Power consumption increase in triangular milling pattern .....	14
<b>Figure 12</b> Power signal matching with simulation.....	16
<b>Figure 13</b> Burr formation on milling done with worn tool .....	16
<b>Figure 14</b> Material left due to tool path.....	17
<b>Figure 15</b> Slot milling repeated until tool failure .....	18
<b>Figure 16</b> Shooting angle and view window of optical microscope .....	21
<b>Figure 17</b> Tool wear comparison with optical microscope .....	22
<b>Figure 18</b> Average flank wear of tool for measured and	

calculated power consumption .....	23
<b>Figure 19</b> Algorithm for tool wear monitoring .....	25
<b>Figure 20</b> Slot milling with cutting conditions changed during process.....	26
<b>Figure 21</b> Threshold model for a changing cutting conditions during a milling process.....	27
<b>Figure 22</b> Simple model of an SVM .....	29
<b>Figure 23</b> Power consumption of slot milling process with various degrees of tool wear .....	29
<b>Table 1</b> Sample data of tool with flank wear of 0.04 mm and sample time frame.....	30

# Chapter 1. Introduction

## 1.1. Study Background

Metal cutting operations benefit from tool condition monitoring systems (TCMS) in a variety of ways [1]. It allows the diagnosis of current tool state and therefore the estimation of important factors such as surface quality. It can also be used to predict and prevent tool failure preventing possible damage done to the product, or worse, the machine itself.

Approximately 7–20% of total milling–machine downtime is caused by tool failure [2–3] and 3–12% of total processing cost comes from tool change costs [10]. In addition, indirect costs due to poor surface quality can add to the total manufacturing costs in the absence of such a monitoring system. Overall, it is estimated that successfully detecting tool breakages can save up to 40% of production costs [11].

Many studies have been performed trying to develop an accurate, reliable, and cost–effective TCMS. TCMS can be categorized into two main group: direct methods and indirect methods.

Direct methods implement devices such as touch trigger probes and optical sensors to directly monitor tool status. The advantages of using direct methods are that they are very accurate when monitoring conditions are ideal and without hindrances. The downsides are the high implementation costs of both equipment and software. It is also difficult to devise a real–time method of modeling tool wear because of the difficulties in

accessing the tool during the machining process. The difficulties in detecting tool wear in the presence of chips or cutting fluid on the tool surface also pose a challenge [4].

Indirect TCMS try to overcome these problems by implementing ways to monitor tool wear without direct monitoring of the tool. This allows real-time tool wear monitoring that is not affected by the unavoidable existence of chips and/or cutting fluids during machining. Additional advantages of indirect methods are the low cost and adaptability of the systems. The downsides would be the difficulties in analyzing and processing the indirect data and finding connections to the actual tool wear, hence the wide-spread use of machine learning systems.

Indirect methods include the measurement of cutting force, vibration, motor current, or acoustic emissions [2, 5–9]. Vetrichelvan, G., et al [2] used acoustic sensors in a turning operation to find the relationship between acoustic emission and tool wear. A genetic algorithm was also proposed to categorize worn and usable tools according to the preset tool wear criterion. A.I. Azmi [5] studied the effects of tool wear on feed force while performing milling processes on glass fiber reinforced composites (GFRP). The study also proposed an adaptive network-based fuzzy inference system to infer the wear on the tool during machining. A. H. Ammouri [6] studied the versatility of the current rise criterion by measuring the spindle current while processing carbon steel. Danko, B., et al [13] proposed an analytic fuzzy classifier and support vector machine without constraints on the number of features in the machining process used for training. Young-Sun Hong et al [21] proposed a tool monitoring system for micro-end milling using wavelet packet

transform of force and torque signals.

Recently developed systems utilizing motor current measure the current consumption of the main spindle. When tool wear occurs, cutting force is increased, causing a rise in current consumption of the motor. Although a reliable and cost-effective method, the actual implementation of the system on machines already in use can have some issues such as down time and refusal of after-service repairs if the machine is tampered with. By measuring the main power of a machine, one can achieve similar results from measuring the input current of the spindle motor without its downsides.

## 1.2. Purpose of Research

The purpose of this study is to build a low-cost, wireless monitoring system that is easy to deploy with little implementation downtime and propose a model that can monitor tool wear by measuring the total power consumption of the CNC milling machine processing aluminum. Aluminum is a ductile material that deforms more easily than other common materials used, such as carbon steel or wood. It is neglected in many studies due to the difficulties in processing the material because of its ductile property. This study aims to explore the effects of tool wear on a milling process while machining aluminum and propose a model for tool wear through the measurement of the total power consumption of the CNC machine. By using the total power consumption, the study hopes to overcome the practical difficulties in implementing conventional TCMS models using spindle power consumption. Through this model, a low-cost method of predicting the tool wear of a CNC milling machine processing aluminum can be suggested.

# Chapter 2. Hardware

## 2.1. System Layout

The system was developed as an external module for ease of installation on machines already in use. A Hall-effect sensor (Winson WCS6800, South Korea) and voltage sensor (Autonics MT4Y-AV-43, South Korea) was used to measure the power consumption of a 5-axis CNC Machine (Hyundai Tech. Corp. CE6405E-5X, South Korea). The data was collected by an Arduino MKR1000 and sent to a subscriber via Wi-Fi. A Message Queuing Telemetry Transport (MQTT) protocol mosquitto was used for fast data transfer. The current sensor had a sensitivity of 65 mV/Amp and a sensing range of 0 to 35 A. The voltage meter had a sensing range of 0 to 500 V and an accuracy of  $\pm 0.3\%$  with a sampling cycle of 16.6 ms for data transmission to the Arduino. The Arduino MKR1000 uses an analog-to-digital converter (ADC) with a 12 bit resolution.

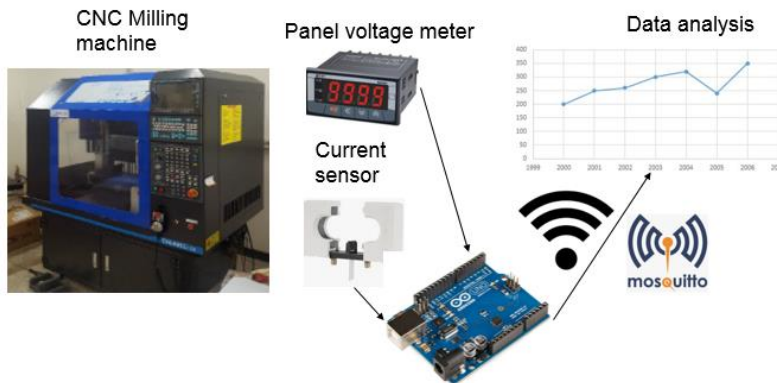
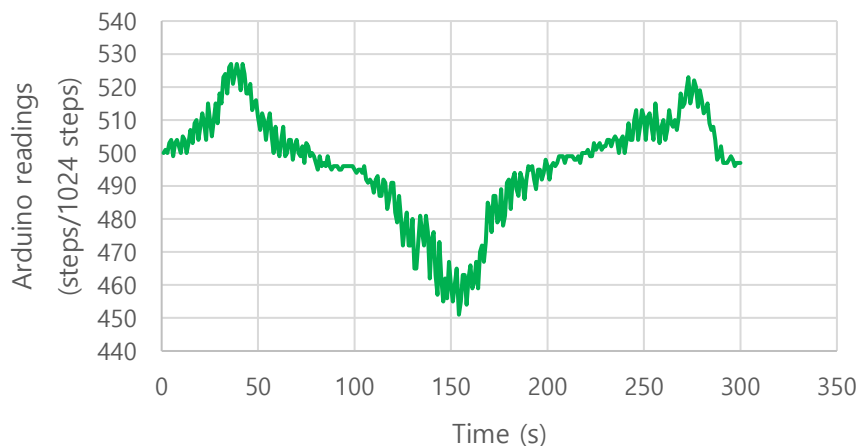


Figure 1 Monitoring system layout

## 2.2. System Design

The Hall-effect sensors used for measuring current in this study are cheap and easy to use due to their clip-on design, requiring no downtime. However, they are very noisy and need filtering for valid data. Figure 2 shows how error-prone a Hall-sensor reading can be. The measurement was taken from a 220 V, 60 Hz power supply. As you can see, the sensor reading values are very noisy and applying root-mean-squared (RMS) to the values directly would not give any meaningful results. Several measures were taken to deal with this problem.

First, a small capacitor ( $0.1 \mu\text{F}$ ) was connected to deal with the high-frequency noise. Since impedance of a capacitor decreases with the increase of frequency ( Impedance  $Z = 1/2\pi fC$  ), high frequency current will flow through the capacitor, not to the Arduino.



**Figure 2 Noisy Hall-sensor readings by Arduino of 220 V 60 Hz power supply**

Second, the wires for providing power to the Hall sensor and the wires for receiving data were electromagnetically shielded with a grounded aluminum foil. Long wires for sending and receiving data act as antennae that capture random electromagnetic waves present everywhere. If installed near electrical components, all sensitive wiring needs shielding. Since the sensors were installed near a large CNC machine and most importantly an Arduino sending data through Wi-Fi, random electromagnetic waves were bound to be abundant in the proximity of the sensor wires. It was crucial that they were suitably shielded. Figure 3 shows how the current sensors are connected to the Arduino.

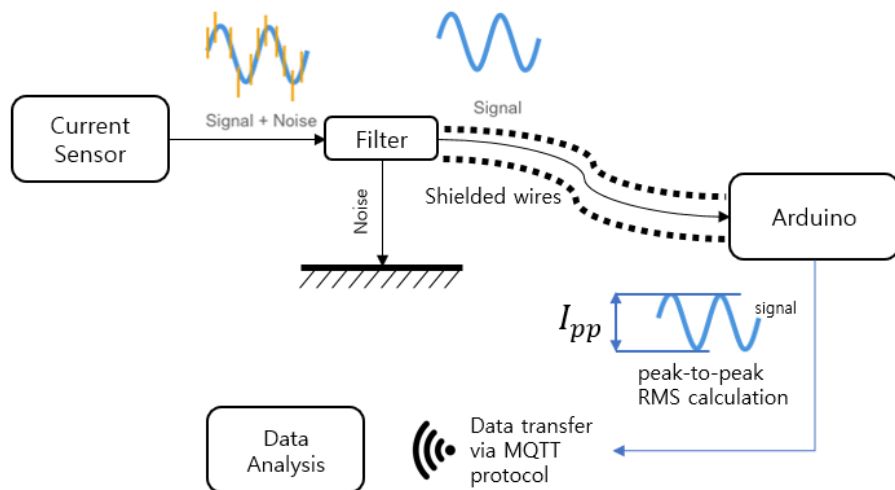


**Figure 3 Model for Arduino-based monitoring system**

Third, the algorithm for receiving data on the Arduino was refined to compensate for the low computational power of the Arduino. The reason for choosing the Arduino MKR1000 was because of the ease of implementation into any situation and the

low-price range the Arduino series offers. The drawback was the low computational power and low sampling rate that comes with the result of it. To counter this, the algorithm for collecting data from the sensors were designed to perform the least amount of calculations for speed and save the least amount of data before sending the dataset to the MQTT server. The Arduino first takes samples for a set time window as fast as possible without any calculations to minimize the time interval between samples. Then the minimum and maximum values were selected for each sensor during that time frame. The difference between the maximum and the minimum values, otherwise called peak-to-peak current was then multiplied by an RMS constant. Then the data was sent via MQTT to a server. This way, when the Arduino takes samples from the sensor, the Arduino does no calculations other than take values from the analog-to-digital converter (ADC). When the Arduino is calculating RMS, the Arduino needs only the peak-to-peak values, minimizing data that needs to be processed and reducing calculation time. A sample of 100 values per sensor were taken for each sample set, and around 5 sample sets were sent via Wi-Fi every second.

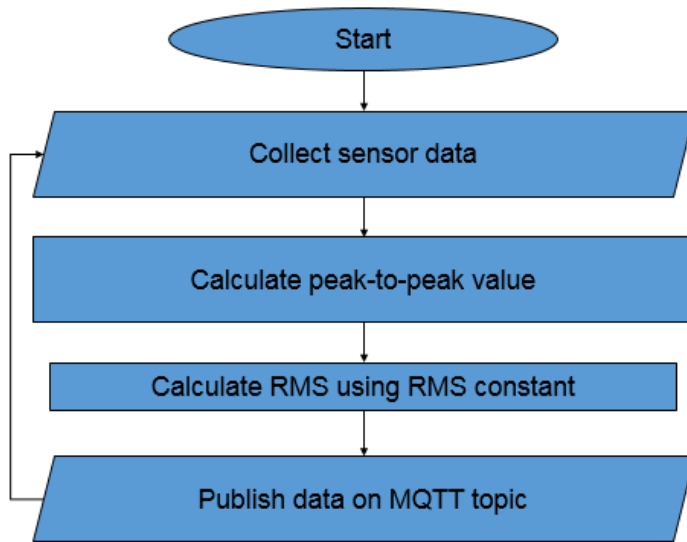


Figure 4 Optimized algorithm for Arduino

Assuming a pure sinewave, the RMS constant is  $\sqrt{2}$ . However, this is rarely true. The RMS constant was calibrated using measurements with a conventional power monitoring system. To verify the accuracy of the system and calibrate the RMS constant, the setup was compared with a Lab-View setup linked to a CD-300 current transducer and a Siemens Sentron PAC3200. A spindle spinning at various speeds and with various loads was monitored for comparison. Figure 5 compares the measurements made with both systems. A mean percentage error of approximately 0.6% (excluding overshoot caused by sudden power surge at power on and power off) was achieved.

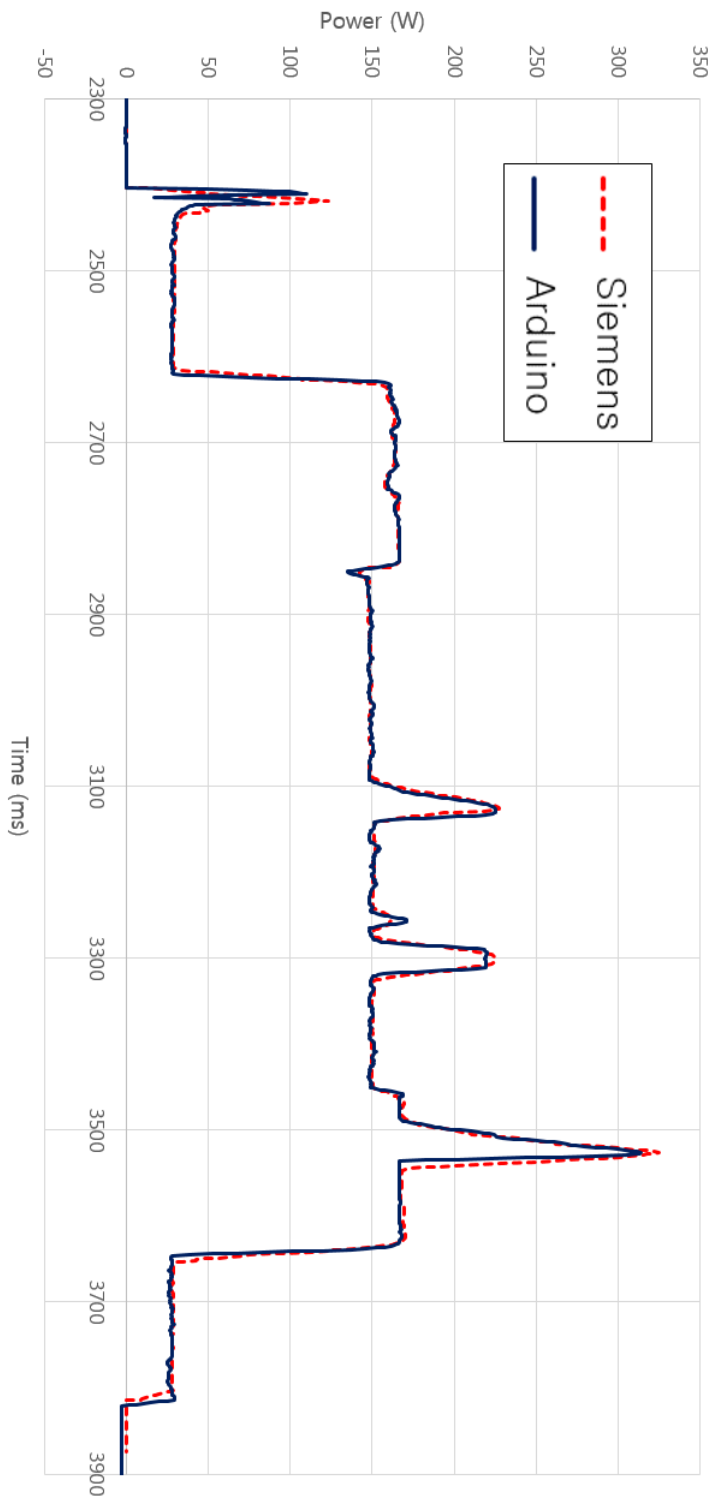


Figure 5 Comparison between Siemens and Arduino monitoring systems for accuracy

A MQTT protocol was used to send data from the Arduino to a receiver for data analysis. MQTT is a light-weight messaging protocol without heavy headers to hinder speed and thus is more forgiving when it comes to required specifications, perfect for use on an Arduino [14]. MQTT works by establishing a broker that handles all incoming and outgoing messages through a system called a broker pattern. A publisher can create a 'topic' and publish messages to that 'topic'. A subscriber can subscribe to any 'topic' that a publisher created proving the subscriber has user authentication. A broker collects all the incoming messages according to their 'topic' and sends the data to all the subscribers currently subscribed to that specific 'topic'. Since multiple publishers and subscribers can publish and subscribe respectively to the same to the same topic, MQTT is suitable for large communication networks that have limited computational resources such as the internet of things (IOT) and for this study. Figure 6 shows how MQTT can be used for multiple monitoring systems in the case of implementation at factories to monitor tool wear.

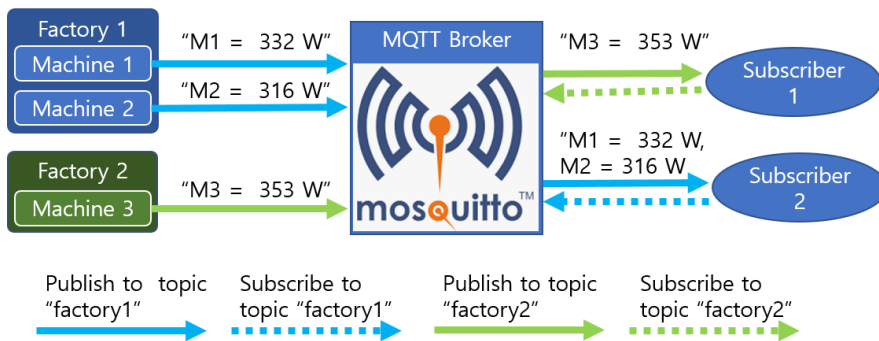


Figure 6 Example of a MQTT protocol

# Chapter 3. Experiments and Results

## 3.1. Early Experiments

Milling experiments were carried out on a 5-axis CNC Machine CE6405E-5X. High-speed-steel (HSS) Co 8% 2F end mill ( $\phi$  6 mm) was used to make cuts on an Al 6061 block. Spindle speed was 12000 RPM, feed was 2000 mm/min, and depth of cut was 1 mm. A slot 6 mm wide and 100 mm long was made with a new tool and a worn tool and the power consumption using the two were compared. A similar test was performed cutting triangular shapes on an aluminum block simulating a manufacturing process of an actual machined part. The spindle speed was 12000 RPM, feed was 1200 mm/min, and depth of cut 1 mm. The new tool was worn out by cutting the same triangular shape approximately 30 times.

Power consumed by the CNC machine increased approximately 6.8% with the increase in tool wear in slot milling procedures.

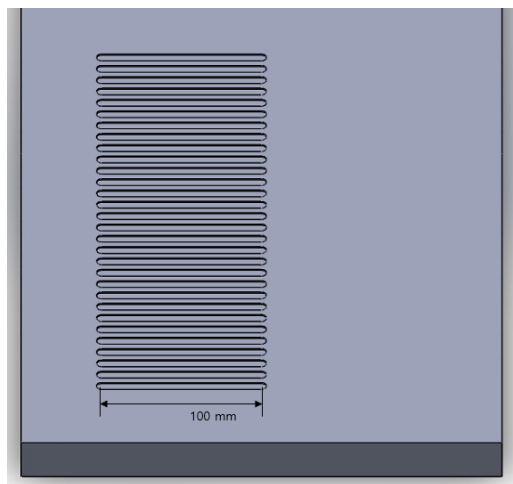
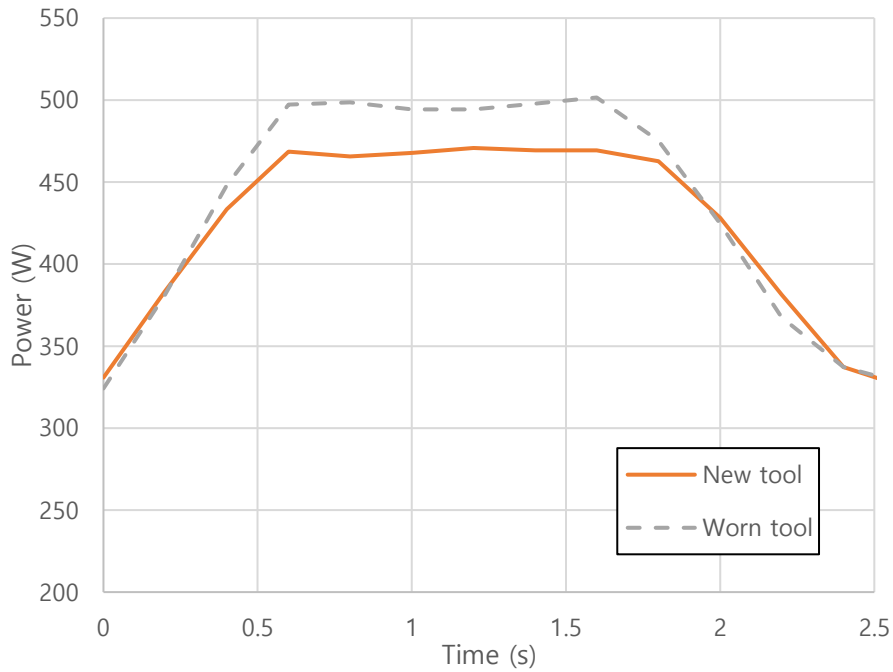


Figure 7 Slot milling process repeated 30 times



**Figure 8 Power consumption increase with tool wear in slot milling**

Meanwhile, the power consumption in the triangular milling pattern increased to 26.3% from the new tool. This large increase may be because in slot milling, the width of cut is always maximum. During triangular milling, in contrast, the width of cut varies as the machining procedure is carried out through the curving and winding toolpath. The decrease in width of cut causes a decrease in power needed for the overall cutting process and thereby increasing the percentage ratio of the worn tool versus the new tool.

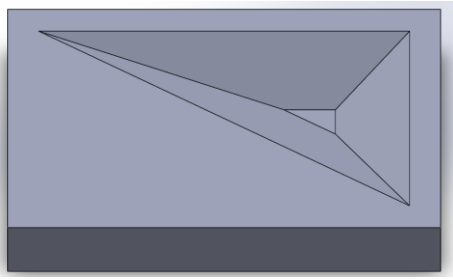


Figure 9 CAD model of triangular cutting experiment

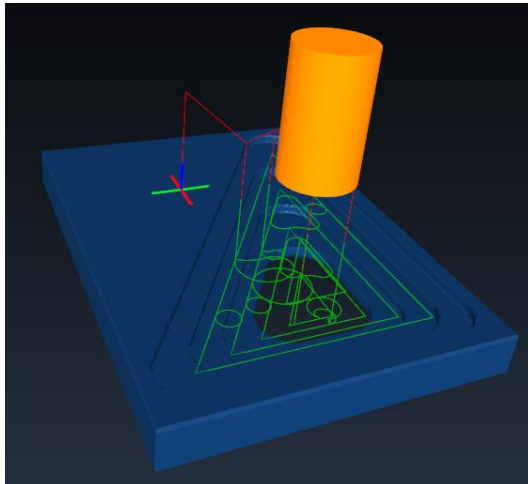


Figure 10 Simulation using CAMotics, a tool path generator

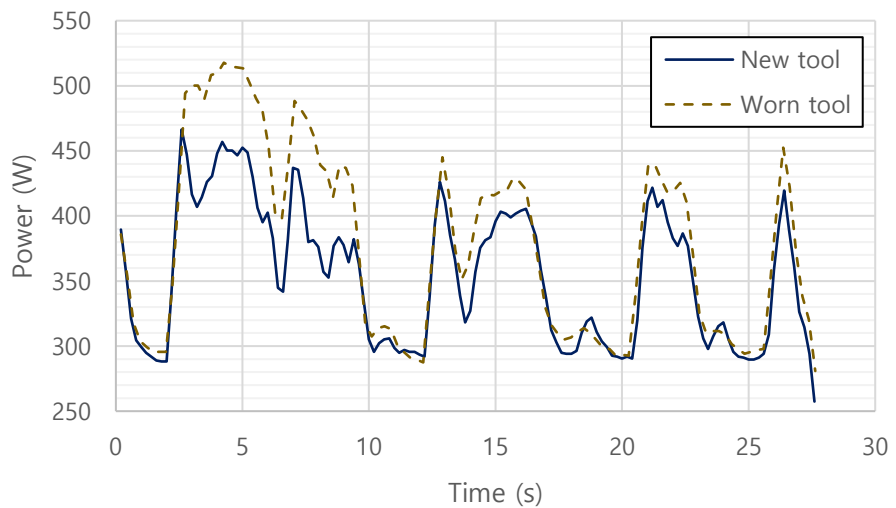


Figure 11 Power consumption increase in triangular milling pattern

To match the actual milling process to the power signal, a G&M code simulation was used to visualize the milling procedure. Figure 10 shows the simulation of tool path created to manufacture the part shown in Figure 9. Figure 12 shows the matching of the power consumption with the milling procedure. A worn tool has higher peaks than a new tool. However, with a quick look at the valleys, it can be observed that the power consumption of an old tool sometimes drops under the power consumption of a new tool. The reason for this can be deduced with the simulation results.

There are four main peaks of power for four step-downs in the process. The valleys consist of codes that sweep the surface flattening leftover material after initial cutting of the surface, requiring less material removal and less power consumption, thus creating the valleys. The power consumed during this valley phase is lower with the worn-out tool because the blunt tool pushes material aside causing unclean cuts, therefore leaving less material left after the initial sweep. Figure 13 and Figure 14 shows why this phenomenon occurs.

As shown in Figure 13, an old tool produces more burring than a new tool. This means in Figure 14 the small bit of material left would have experienced burr formation when a worn tool was used, meaning excessive force would have been applied to it [19]. With more force applied to the small bit of material during the initial roughing procedure when using a worn tool, it would be easier to cut away the material in the final sweep, or the valley phase. This, in turn, would cause a decrease in power consumption.

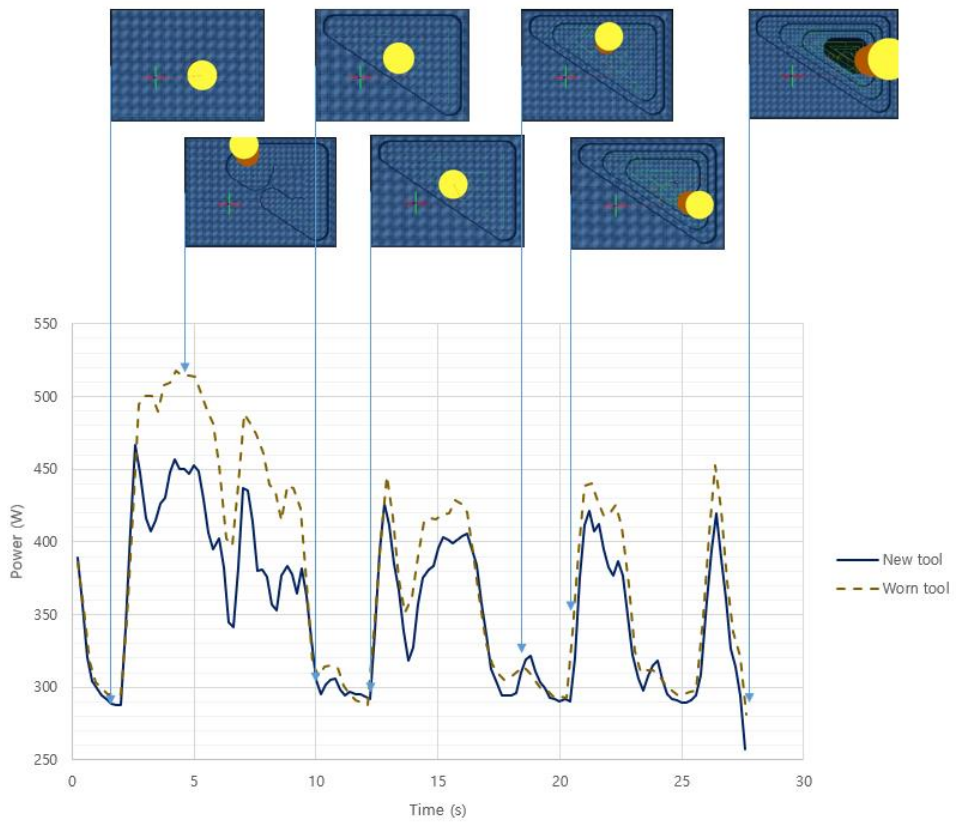


Figure 12 Power signal matching with simulation

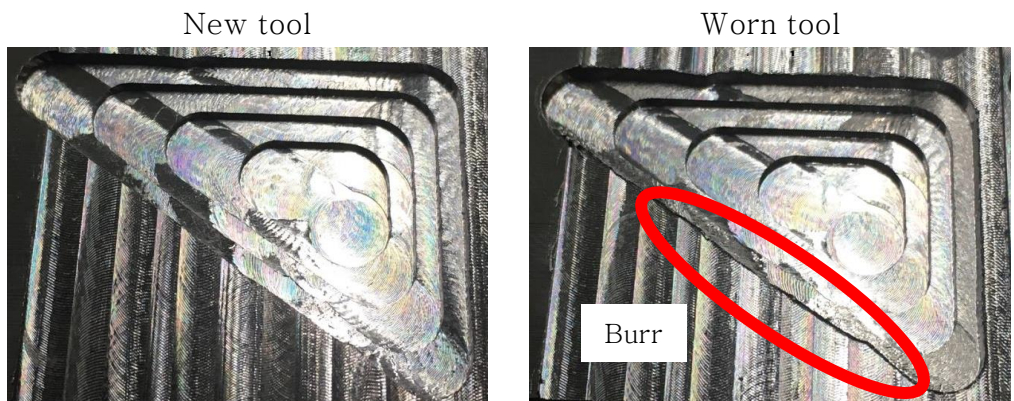


Figure 13 Burr formation on milling done with worn tool

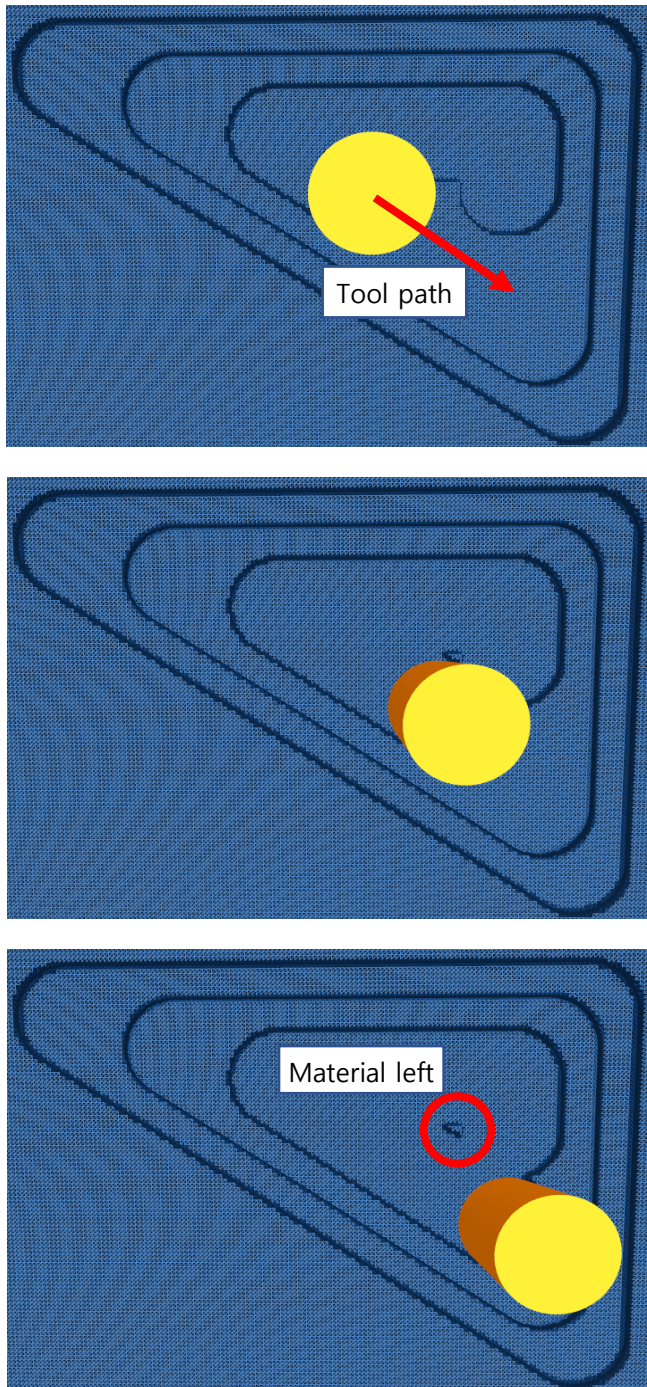
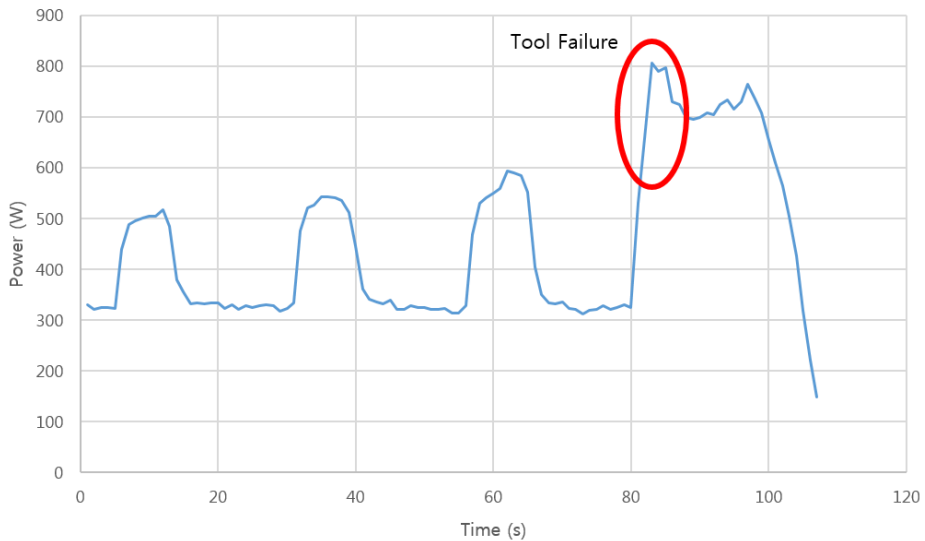


Figure 14 Material left due to tool path

Overall, these results show total power consumption increase with increase in tool wear. In order to verify the results, additional slot milling procedure with the same condition used in Figure 15 Figure 7 was performed until signs of tool failure was detected.



**Figure 15 Slot milling repeated until tool failure**

Tool failure caused approximately 70% increase in power consumption and the procedure just before the failure occurred had an increase of 19.07%. An overall increase in the power consumption due to tool wear suggests measuring the total power consumption of the CNC milling machine can be a viable strategy in tool condition monitoring. The sudden increase in power consumption during tool failure suggests the ease of which tool failure can be detected using the total power consumption of the machine.

## 3.2. Mathematical Model

To attempt a mathematical approach for designing a tool wear monitoring system, a spindle power model for tool wear monitoring was used to see if the model works for the main power instead of the spindle power. A study done by H. Shao [7] shows power needed for the spindle can be calculated by using the cutting conditions, hardness of the work-piece, mean chip thickness, chip thickness constant, sliding friction between the workpiece and the tool, cutting force constant, the number of cutting teeth, angle of cutting tooth ant entry and exit, the immersion angle, and the average flank wear of the tool. The following equation from the study shows the power needed for the spindle when tool wear is present.

$$\bar{P} = \frac{ZnDa_p [K\bar{h}^{(-c)}f_z(\cos(\varphi_{in}) - \cos(\varphi_{in} + \psi)) + \mu H\bar{V}\bar{B}\psi]}{2}$$

- $Z$  = number of cutting teeth
- $n$  = spindle speed
- $D$  = diameter of milling cutter
- $a_p$  = depth of cut
- $K$  = cutting force constant
- $\bar{h}$  = mean chip thickness
- $c$  = chip thickness constant
- $f_z$  = feed rate per tooth
- $\varphi_{in}$  = angle of cutting tooth at entrance

- $\varphi_{out}$  = angle of cutting tooth at exit
- $\psi$  = immersion angle
- $\mu$  = sliding friction coefficient between work-piece and tool
- $H$  = Brinell hardness of work-piece
- $\overline{VB}$  = average flak wear width

The values used for the equation are

- $Z$  = 2
- $n$  = 12000 RPM
- $D$  = 6 mm
- $K$  = 400 N/mm<sup>2</sup>
- $c$  = 0.147
- $\bar{h}$  = 0.35 mm
- $H$  = 80 Brinell
- $f_z$  = 1/12 mm/tooth
- $\varphi_{in}$  = 0
- $\varphi_{out}$  =  $\pi$
- $\psi$  =  $\pi$
- $\mu$  = 0.54

The average flank wear of the tool was measured using a microscope. Figure 16 shows how the average flank wear was measured. Figure 17 shows a comparison between a new tool, a worn tool, and broken tool under a microscope.

The new tool is very clean with fine edges. In contrast, the flank wear is clearly visible on the worn tool with due to the different reflecting angle of the light source of the microscope. The tool that failed clearly has a broken edge that hinders the machining process and most definitely is the cause of the spike in power consumption.

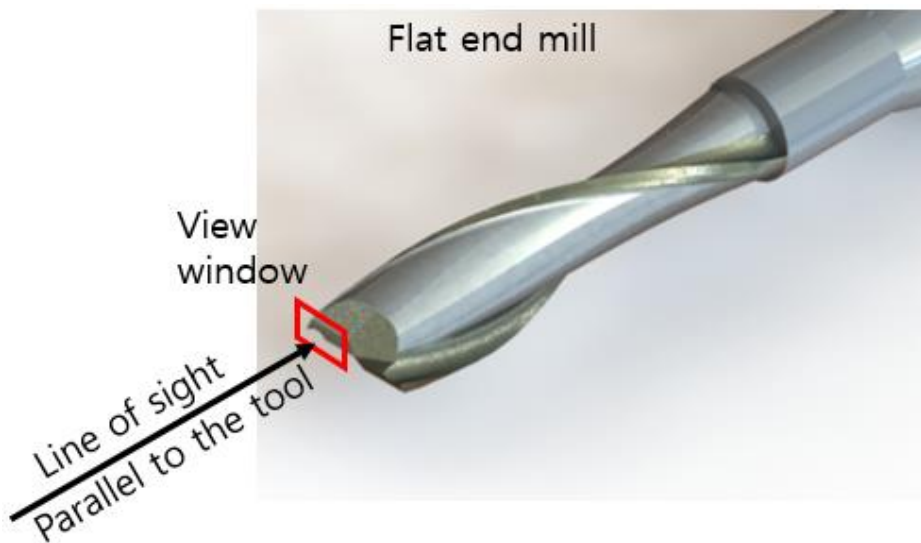
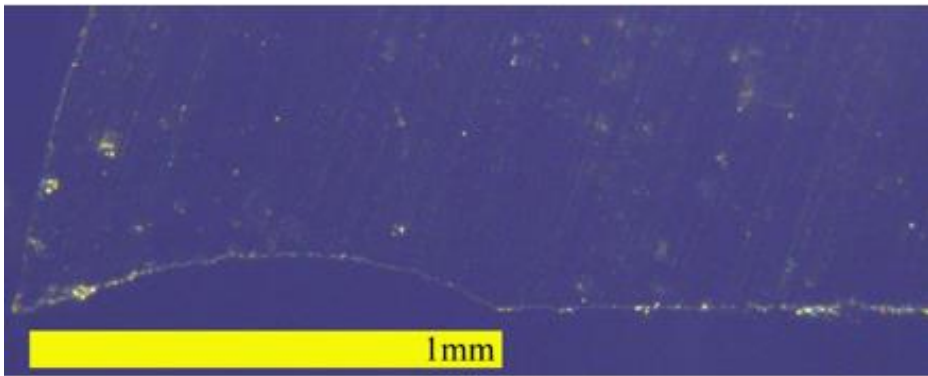
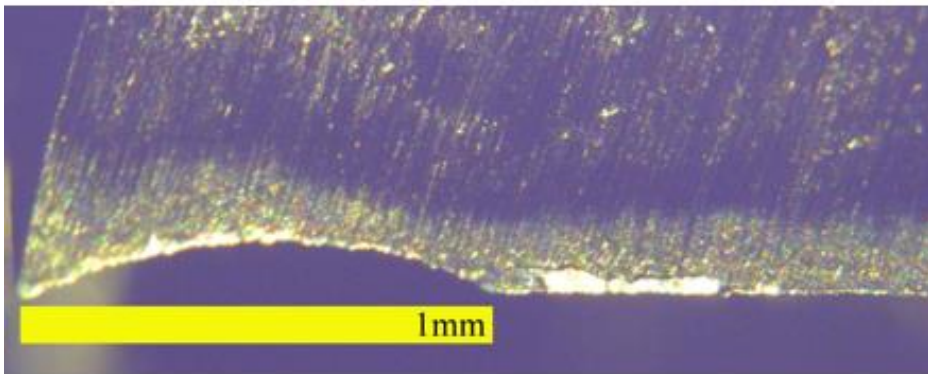


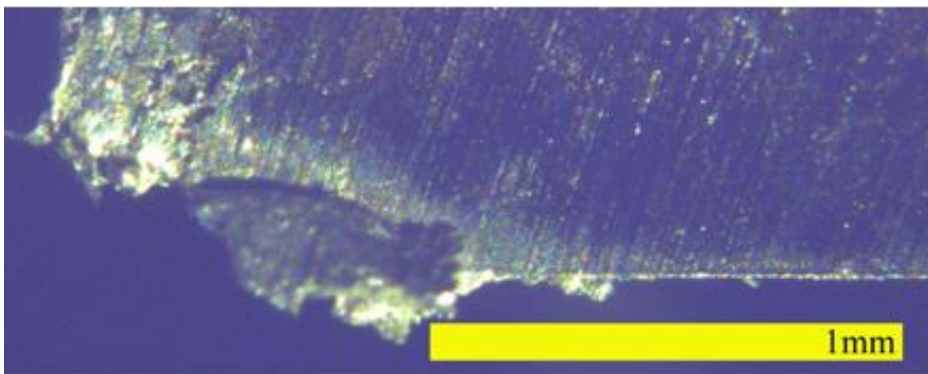
Figure 16 Shooting angle and view window of optical microscope



**New tool**



**Worn tool**



**Tool failure**

Figure 17 Tool wear comparison with optical microscope

Power consumption calculated according to the equation was compared with experimental data. Since the equation only represented power consumption of the spindle, the idle power of the machine had to be subtracted from the measured data. Also, the power increase in the servo motors for X, Y, and Z axial motion had to be compensated for. Figure 18 shows a comparison between the measured and calculated power consumption according to the average flank wear of the tool after the idle power of the CNC machine was subtracted from the measured value. An average of 5% error due to the increase in power consumption of the servo motors was observed.

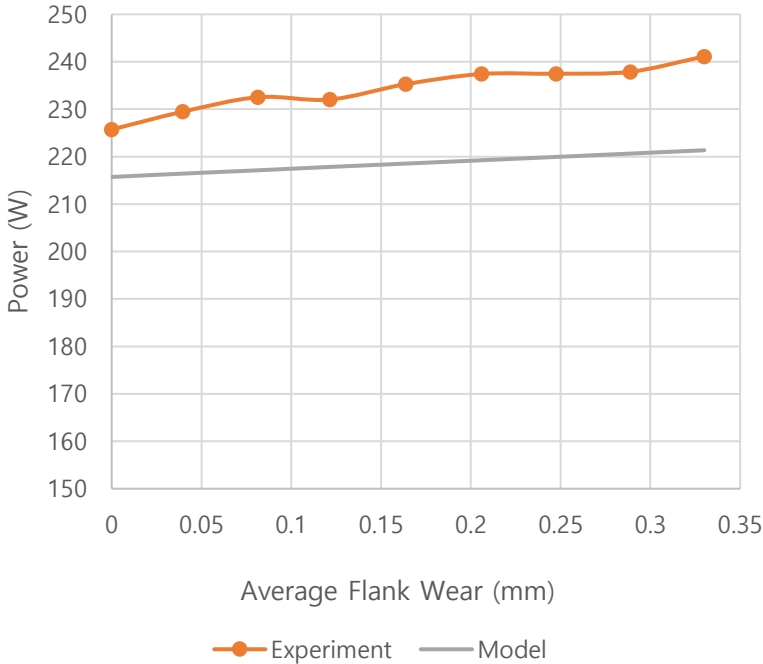


**Figure 18 Average flank wear of tool for measured and calculated power consumption**

With this, the following model can be proposed to classify a worn tool and a usable tool. First, considering product quality requirements, for example surface quality and dimensional accuracy, a tool wear criterion is selected. The maximum allowable average flank wear ( $\overline{VB}$ ) is set. The cutting conditions of the milling process is used to calculate the spindle power needed for the specific operation by using the equation from H. Shao [7]. Since this system only measures the main power, and not the spindle power, the calculated power is compensated for by adding the idle power and the 5% offset due to the increase in power consumption of the X, Y, and Z servo motors. This calculated value is now the threshold power. After measuring the actual power consumption of the machine during the specific milling process, the threshold power is compared to the measured power. If the measured power is larger than the calculated power, a warning can be issued to inform the observer of the worn-out state of the tool in use. If the cutting conditions change during the milling process, the threshold power is calculated again using the updated conditions, and the loop starts again.

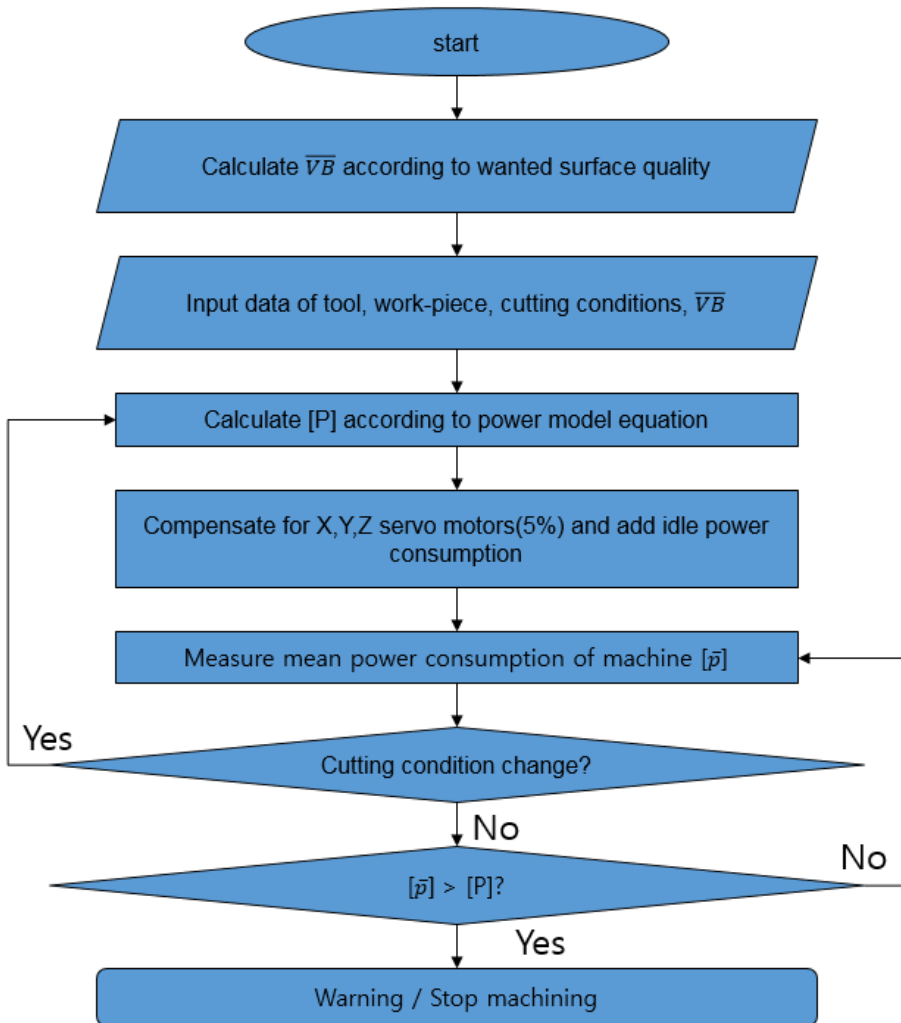
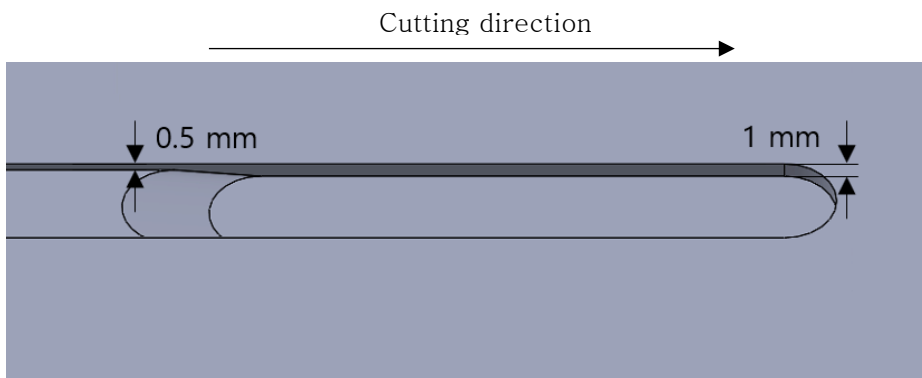


Figure 19 Algorithm for tool wear monitoring

To verify the algorithm, cutting conditions during a milling process was changed to make sure the model holds for the changes made while the process is performed. Figure 21 compares the power consumption of a cut made with a worn-out tool and a new tool when the condition changes during the process. The old tool had an average tool wear of 0.89 mm. The cut width was 6 mm and the depth 0.5 mm. The tool wear criterion was chosen to be 0.5 mm. The depth of cut was changed to 1 mm at the 3 second mark. As observed, the model corrects itself at the 3 second mark according to the spindle power model and compensates for the idle power and the X, Y, and Z motors. Although the model holds for the changes in cutting conditions, it separates the worn-out tool from the new tool by a narrow margin.



**Figure 20 Slot milling with cutting conditions changed during process**

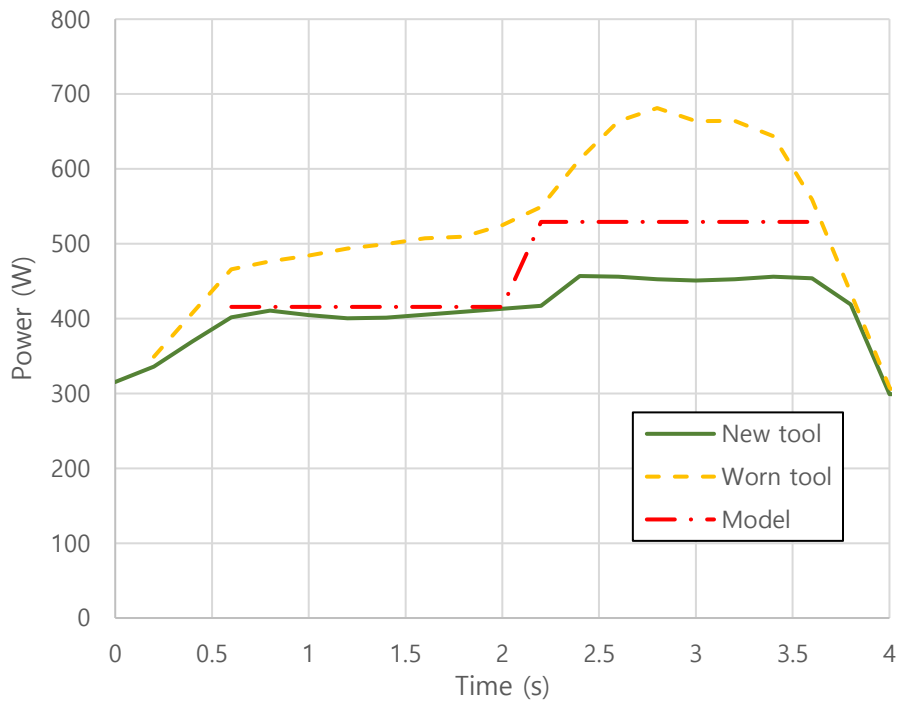


Figure 21 Threshold model for a changing cutting conditions during a milling process

### 3.3. Machine Learning Model

To propose a more reliable tool monitoring system, a Support Vector Machine (SVM) was trained and used to predict tool wear and categorize tools with power consumption data. A SVM, initially conceived of by Cortes and Vapnik [17], is mostly used for classification and regression. The objective of an SVM is to create a hyperplane to separate the data so that the hyperplane is as far as possible from the closest members of both classes [17–18, 20, 22]. Figure 22 shows a simple model of an SVM with linearly separable classes that explains how SVMs work. The SVM first tries to change the orientation of the hyperplane so that the margin is maximum. The closest members of both classes to the hyperplane are deemed support vectors.

To prepare the dataset, slot milling process was performed using tools with 7 different degrees of average flank wear. Each slot was 6 mm wide and 0.5 mm deep. The average flank wear was measured using an optical microscope. Figure 23 shows the average, minimum, and maximum power consumed by the machine during slot milling when using tools with varying degrees of flank wear.

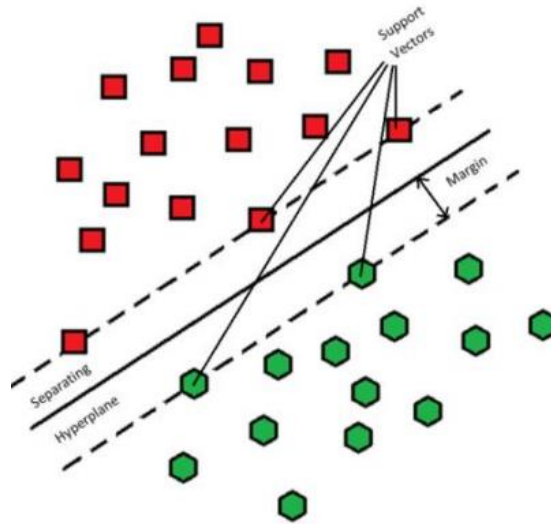


Figure 22 Simple model of an SVM [22]

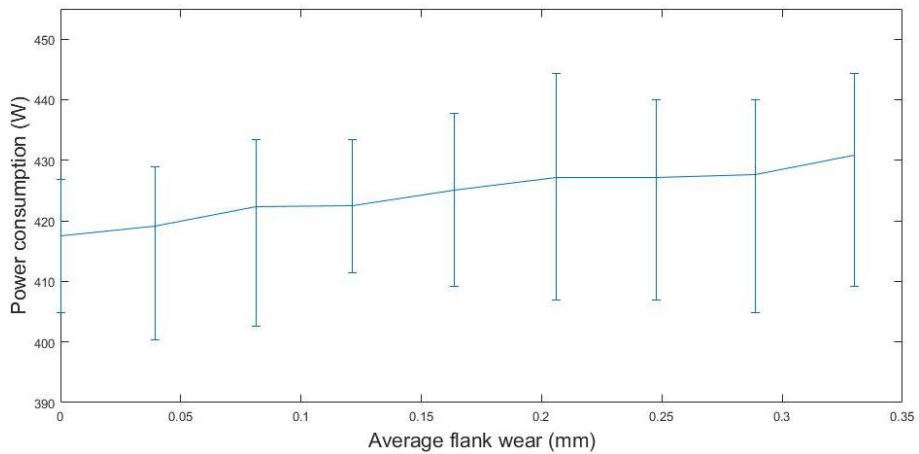


Figure 23 Power consumption of slot milling process with various degrees of tool wear

To train the SVM, the acquired dataset was first labeled with the degree of flank wear and whether the tool was performing a cut or not. The dataset was categorized into 3 parts: power consumption in-between cuts (idle), a tool with average flank wear below 0.2 mm (classified as “good tool” ), and a tool with average flank wear above 0.2 mm (classified as “bad tool” ).

Because the instantaneous power consumption ( $P_n$ ) alone was not enough to train the SVM, several other input sets were used. 5 consecutive values on the time scale ( $P_{n-4}, P_{n-3}, P_{n-2}, P_{n-1}, P_n$ ) were used to gather average, minimum, maximum, and standard deviation values of power consumption of that time frame. Table 1 shows an example of a dataset and an example of a timeframe for calculation of the statistical values.

Also, the derivative values ( $\frac{P_n - P_{n-1}}{\Delta t}$ ) were used to factor in the rate of change of the power consumption. An Accuracy of 81.84% was achieved. Although this is a relatively low value, this can be compensated for by using the consecutive results on the time frame. If correctly identifying one sample is 81.84%, correctly identifying 3 samples out of 5 samples becomes 95.63%.

**Table 1 Sample data of tool with flank wear of 0.04 mm and sample time frame**

	Power	minimum	maximum	average	stddev	f'	f''	Classification
	292.6	292.6	308.0	299.6	7.684	-11.83	-63.59	idle
	288.2	288.2	308.0	295.7	7.395	-23.40	-61.58	idle
	292.6	288.2	294.8	292.6	2.694	23.53	251.0	idle
	288.2	288.2	294.8	291.3	2.951	-23.66	-253.7	idle
	407.0	288.2	407.0	313.7	52.19	560.4	2755	good tool
$P_{n-4}$	420.2	288.2	420.2	339.2	68.07	70.59	-2619	good tool
$P_{n-3}$	424.6	288.2	424.6	366.5	69.81	23.28	-250.3	good tool
$P_{n-2}$	422.4	288.2	424.6	392.5	58.70	-11.76	-187.4	good tool
$P_{n-1}$	420.2	407.0	424.6	418.9	6.887	-11.76	0	good tool
$P_n$	422.4	420.2	424.6	422.0	1.840	11.70	124.8	good tool

### 3.4. Summary

In order to propose a model for the monitoring of tool wear, milling processes of simple dimensions were carried out with both a new tool and a worn-out tool to observe the effect of tool wear on the main power consumption of a 5-axis CNC milling machine. The main power consumption of the machine was measured using system of sensors connected to an Arduino. The data was sent to a server via Wi-Fi using MQTT protocol. A G&M code simulator was used to simulate and match the milling process with the power consumption data. A model based on physical modeling and a model based on machine learning was proposed and checked for validity.

## Chapter 4. Conclusions

In this thesis a low-cost wireless monitoring system with little to no implementing down time that can be used as a tool condition monitoring system was developed. The possibility to use total power consumption of the CNC milling machine to diagnose tool condition was explored. A mathematical model was used and compared with experimental data to develop an algorithm for tool wear monitoring. Also, an algorithm to train a support vector machine to measure tool wear was proposed and tested.

## Reference

- [1] Rizal, M., et al. (2014). A Review of Sensor System and Application in Milling Process for Tool Condition Monitoring. *Research Journal of Applied Sciences, Engineering and Technology* 7: 2083–2097.
- [2] Vetrichelvan, G., Sundaram, S., Kumaran, S. S., & Velmurugan, P. (2015). An investigation of tool wear using acoustic emission and genetic algorithm. *Journal of Vibration and Control*, 21(15), 3061–3066.
- [3] Bhattacharyya, P., Sengupta, D., Mukhopadhyay S. (2007). Cutting force–based real–time estimation of tool wear in face milling using a combination of signal processing techniques, *Mechanical Systems and Signal Processing*, Volume 21, Issue 6 , Pages 2665–2683.
- [4] Drouillet, C., et al. (2016). Tool life predictions in milling using spindle power with the neural network technique, *Journal of Manufacturing Processes*, Volume 22, Pages 161–168, ISSN 1526–6125.
- [5] Azmi, A.I., (2015). Monitoring of tool wear using measured machining forces and neuro–fuzzy modelling approaches during machining of GFRP composites. *Adv. Eng. Softw.* 82, C (April 2015), 53–64.

- [6] Ammouri, A., Hamade, R. (2014). Current rise criterion: a process-independent method for tool-condition monitoring and prognostics. *Int J Adv Manuf Technol* 72(1-4):509-519 36.
- [7] Shao, H., Wang, H., Zhao, X. (2004). A cutting power model for tool wear monitoring in milling. *Int J Mach Tools Manuf* 44(14):1503- 1509 37.
- [8] Ritou, M., Garnier, S., Furet, B., Hascoet, J. (2014). Angular approach combined to mechanical model for tool breakage detection by eddy current sensors. *Mech Syst Signal Process* 44(1-2):211-220 38.
- [9] Sevilla, P., et al. (2011). Tool breakage detection in cnc high-speed milling based in feed-motor current signals. *Int J Adv Manuf Technol* 53(9-12):1141-1148
- [10] Liu, C., Wang, G., Li, Z., (2015). Incremental learning for online tool condition monitoring using ellipsoid ARTMAP network model. *App Soft Comput* 35:186-198
- [11] Cho, S., Asfour, S., Onar, A., Kaundinya, N. (2005). Tool breakage detection using support vector machine learning in a milling process, *International Journal of Machine Tools and Manufacture*, Volume 45, Issue 3, Pages 241-249, ISSN 0890-6955,

- [12] List, G., et al. (2005). Wear behaviour of cemented carbide tools in dry machining of aluminium alloy, Volume 259, Issues 7–12, Pages 1177–1189, ISSN 0043–1648,
- [13] Danko, B., et al. (2010). Tool wear estimation using an analytic fuzzy classifier and support vector machines. *Journal of Intelligent Manufacturing*. 23. 1–13.
- [14] Thangavel. D., et al. (2014). Performance evaluation of MQTT and CoAP via a common middleware. Ninth International Conference on Intelligent Sensors, Sensor Networks and Information Processing (ISSNIP). Symposium on Sensor Networks. 21–24 April.
- [15] Kim, D., et al. (2018). Smart Machining Process Using Machine Learning: A Review and Perspective on Machining Industry. *International Journal of Precision Engineering and Manufacturing–Green Technology*. Volume 5. Issue 4. Pages 555–568.
- [16] Lee, G., et al. (2018). Machine health management in smart factory: A review. *Journal of Mechanical Science and Technology*. Volume 32. Issue 3. Pages 987–1009.
- [17] Cortes, C., Vapnik, V. (1995). Support–Vector Networks. *Machine Learning*. Volume 20. Issue 3. Pages 273–297.

[18] Cristianini, N., Shawe–Taylor, J. (2000). An introduction to support Vector Machines: and other kernel–based learning methods. Cambridge University Press, New York, NY, USA

[19] Pena, B., et al. (2005). Monitoring of drilling for burr detection using spindle torque. International Journal of Machine Tools and Manufacture. Volume 45. Issue 14. Pages 1614–1621.

[20] Hameed, Z. (2008). Multivariate analysis for fault detection and classification with Support Vector Machines (SVMs) and Self–Organizing Maps (SOMs) by using statistical time domain features for rolling element bearings. Seoul National University. Master’s Thesis.

[21] Hong, Y.S., et al. (2016). Tool–wear monitoring during micro–end milling using wavelet packet transform and Fisher’s linear discriminant. International Journal of Precision Engineering and Manufacturing. Volume 17. Issue 7. Pages 845–855

[22] Ashour. M. W., et al. (2015). Machining Process Classification using PCA–Reduced Histogram Features and the Support Vector Machine. International Conference on Signal and Image Processing Applications (ICSIPA). 7412226.

## 초 록

# 소비전력 측정을 통한 밀링 공정의 가공 모니터링

공구 모니터링은 공구의 상태를 진단하거나 공구의 파괴를 진단, 예측하는 데 필수 요소이다. 밀링 가공의 중단시간 중 7-20%가 공구 파괴로 인한 것이며 공정 비용의 3-12%가 공구 파괴로 인한 비용이다. 그 외에 공구 마모로 인한 품질저하 등 간접적인 비용 또한 공정비용을 증가시키는 요인으로 작용한다. 기존 공구 교체 전략들은 많은 비용을 요하거나 중단시간을 필요로 하여 적용하기 어려운 면이 있다. 본 연구는 외부에 부착할 수 있는 모듈로 CNC 밀링 머신의 총 전력소모를 측정하여 저렴하고 중단시간 없는 무선 모니터링시스템을 제안한다. 이를 위해 간단한 형상의 마모가 진행된 공구와 새 공구를 이용해 밀링 공정을 실행하여 공구 마모가 총 전력소모에 어떻게 영향을 미치는 지 알아보았다. 전력 측정은 전류센서와 전압센서가 연결된 아두이노로 측정을 하였고 측정된 데이터는 MQTT를 이용해 Wi-Fi로 전송되었다. G&M code 시뮬레이션을 이용해 전력 소모 프로파일을 가공공정과 일치시켰다. 수학적 모델링을 이용한 모델과 SVM을 이용한 모델을 제안하고 테스트하였다.

**주요어 :** 소비전력 측정, 공구 상태 모니터링, 밀링 공정

**학 번 :** 2017-26871